Rate-synchrony relationship between input and output of spike trains in neuronal networks

Sentao Wang[1] and Changsong Zhou[1,2,*]

[1]*Department of Physics, Hong Kong Baptist University, Kowloon Tong, Hong Kong*

[2]*Centre for Nonlinear Studies and The Beijing-Hong Kong-Singapore Joint Centre for Nonlinear and Complex Systems (Hong Kong), Hong Kong Baptist University, Kowloon Tong, Hong Kong*

(Received 27 August 2009; revised manuscript received 6 December 2009; published 28 January 2010)

Neuronal networks interact via spike trains. How the spike trains are transformed by neuronal networks is critical for understanding the underlying mechanism of information processing in the nervous system. Both the rate and synchrony of the spikes can affect the transmission, while the relationship between them has not been fully understood. Here we investigate the mapping between input and output spike trains of a neuronal network in terms of firing rate and synchrony. With large enough input rate, the working mode of the neurons is gradually changed from temporal integrators into coincidence detectors when the synchrony degree of input spike trains increases. Since the membrane potentials of the neurons can be depolarized to near the firing threshold by uncorrelated input spikes, small input synchrony can cause great output synchrony. On the other hand, the synchrony in the output may be reduced when the input rate is too small. The case of the feedforward network can be regarded as iterative process of such an input-output relationship. The activity in deep layers of the feedforward network is in an all-or-none manner depending on the input rate and synchrony.

DOI: 10.1103/PhysRevE.81.011917 PACS number(s): 87.18.Sn, 05.45.Xt

I. INTRODUCTION

Two key measures in neuroscience are the firing rate and synchrony between activities of different neurons, which are widely believed to play central roles in information encoding [1]. The two measures are not independent of each other. It has been demonstrated that the correlation between spike trains increases with the firing rate [2,3]. Several recent studies have shown that synchrony can ensure the transmission of temporally precise signals between neuronal networks [4] and bind different features of the same object [5]. To discharge spikes, neurons need to integrate thousands of presynaptic spikes. At the single neuron level, synchronous input results in a linear input-output relationship [6].

In the nervous system, information is processed by one functional group and then transferred to the next groups. The multilayer feedforward network is quite suitable to model such a process including many stages. In such a topological structure, packets of synchronous activities either die out or propagate stably with millisecond precision depending on the initial condition [7]. It has been shown that the noise background has beneficial effects on signal transmission through the feedforward network [8]. When the input to layer 1 is only independent noise, synchrony can develop gradually and the firing rate (the average number of spikes in a long time) can be propagated [9,10]. With noise injected to each layer, the neurons in deep layers can fire more regularly than those in shallow layers [11]. Correlated firings have been widely observed in experiments [12], which have been linked to attention [13], stimulus discrimination [14], and so on.

So far, the existing works point to nontrivial interplay between the firing rate and synchrony in neuronal systems. In uncoupled neurons with correlated noise input, the synchrony in the output spike trains depends on the firing rate [2]. On the other hand, in the feedforward network, totally uncorrelated input can induce synchronized spiking in deeper layers [10]. It is of interest to explore systematically how the transmission of spike trains through the feedforward network depends on both the firing rate and synchrony. Another interesting issue is to investigate whether there exists not fully synchronized state in deep layers different from previous observations [10].

Therefore, here we focus on two issues. The first one is to explore the $2D$ space (firing rate and synchrony) mapping between input and output spike trains of a network without lateral connections. Another one is to investigate how the activity in deep layers is determined by the input parameter of layer 1.

In this paper we generate correlated spike trains by injecting spatially correlated noise to neurons. These correlated firings are then projected to a network which consists of unconnected neurons. We found that when the firing rate and projection strength are large enough, the output of the network exhibits significant correlation even if the input spike trains are weakly correlated, since uncorrelated firings depolarize the membrane potentials of the neurons to near the threshold. With fixed values of input rate and synchrony, the output synchrony increases sharply and then saturates at a large value as the projection strength increases. On the other hand, when the input rate or projection strength is too small, the synchrony in the output can be reduced compared to that from the input. The feedforward network can be regarded as iterations of such a mapping. As a result of the interplay between firing rate and synchrony, the activity of deep layers is in silence or in full synchrony determined by the parameter values.

II. MODEL

In order to generate correlated spike trains, a spatially correlated noise $\eta_i(t)=\sqrt{1-c}\epsilon_i(t)+\sqrt{c}\chi(t)$ [15] is injected

*cszhou@hkbu.edu.hk

into 2000 integrate-and-fire (IF) neurons [16]. $\epsilon_i(t)$ and $\chi(t)$ are all Gaussian white noise; the correlation coefficient c $(0 \le c \le 1)$ sets the relative weight of the common noise. $\sqrt{1-c}\epsilon_i(t)$ represents the independent noise while $\sqrt{c}\chi(t)$ is the shared noise. There exists no recurrent connection between these neurons. The dynamics of these neurons is described by the following equation:

$$\tau_m \frac{dV_i}{dt} = V_{rest} - V_i + I_0 + \eta_i(t). \tag{1}$$

Here τ_m is the membrane time constant, V_i is the membrane potential of the ith neuron, V_{rest} is the resting membrane potential, and I_0 is the external constant input. When the membrane potential V_i reaches threshold value V_{th}, a spike is generated and the membrane potential is reset to the resting potential at which it remains clamped for a 5 ms refractory period. Here τ_m=20 ms, V_{rest}=−60 mV, I_0=9, and V_{th}=−50 mV. For each neuron i,

$$\langle \eta_i(t_1)\eta_i(t_2)\rangle = 2D\delta(t_1 - t_2), \tag{2}$$

while for a pair of neurons i and j,

$$\langle \eta_i(t_1)\eta_j(t_2)\rangle = 2Dc\delta(t_1 - t_2). \tag{3}$$

Here D is the noise intensity. As a result, the averaged firing rate R can almost keep constant with fixed value of the noise intensity D as the input correlation coefficient c changes. That is, the averaged firing rate R can be solely controlled by the value of the noise intensity D.

These correlated spike trains are then projected to a network which consists of 100 IF neurons without recurrent connections. Each neuron in the network randomly receives synaptic inputs from about 100, i.e., 5%, neurons in the group which is used to generate correlated spike trains. The dynamics of this network is described by the following equation:

$$\tau_m \frac{dV_j}{dt} = V_{rest} - V_j + I_j^{syn}. \tag{4}$$

Here I_j^{syn} is the synaptic current of the jth neuron caused by those input spike trains. The synaptic current I_j^{syn} takes the form

$$I_j^{syn} = g\sum_i \sum_k \delta(t - t_i^k), \tag{5}$$

where the sum over i corresponds to a sum on all synapses of the jth neuron and the sum over k corresponds to a sum over spikes arriving at a given synapse. g is the coupling strength.

The population activity of a network is defined as how many percent of all the neurons in the network fire spikes in a moving time window. Here we call it spike time histogram (STH) $p(t)$ [17]. To quantify the synchronization between neurons, we compute the correlation coefficient between the spike trains of a pair of neurons [2]. A long time interval T =40 s is divided into small bins of τ=40 ms and the two

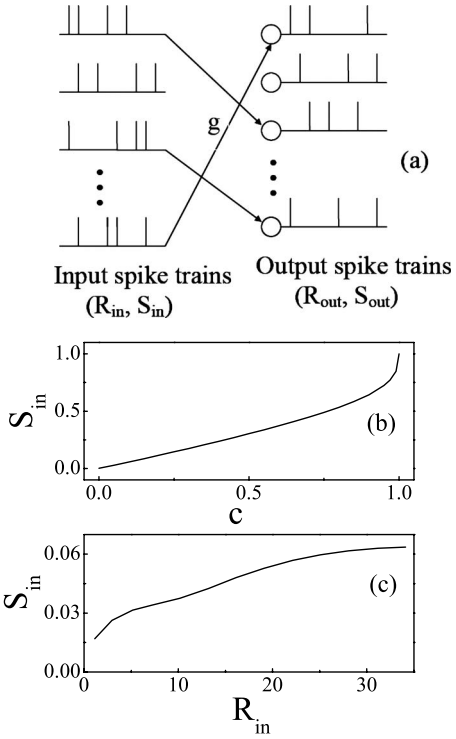

FIG. 1. (a) Schematic illustrating how the input spike trains are transformed by neuronal networks. (b) The input synchrony S_{in} versus the correlation coefficient c with R_{in}=22. (c) The input synchrony S_{in} versus the input rate R_{in} with c=0.1.

spike trains are given by the number of spikes in each time bin, n_1 and n_2. The correlation coefficient is then defined as

$$S = \frac{\langle n_1 n_2\rangle - \langle n_1\rangle\langle n_2\rangle}{\sqrt{(\langle n_1^2\rangle - \langle n_1\rangle^2)(\langle n_2^2\rangle - \langle n_2\rangle^2)}}. \tag{6}$$

S is in the range from 0 to 1. For independent spike trains, S=0. If the spike trains are fully synchronized, S=1. The synchrony degree S of the whole network is obtained by averaging over all pairs of the neurons in the network. The spike trains are characterized by the averaged firing rate R and the synchrony degree S, R_{in} and S_{in} for the input spike trains, and R_{out} and S_{out} for the output spike trains. The scenario is outlined schematically in Fig. 1(a). Since the bin size used to compute the input synchrony S_{in} is the same as that used to compute the output synchrony S_{out}, the reported results do not depend on the length of the time bin qualitatively. Figure 1(b) shows the input synchrony S_{in} versus the correlation coefficient c with R_{in}=22. The input synchrony S_{in} depends on both the input rate R_{in} and the correlation coefficient c. It was found that the correlation between neural spike trains increases with the firing rate as the value of c is fixed [see Fig. 1(c)], which arises from the nonlinearities in the transfer function of the neurons [2]. Whether the neurons fire regularly or highly irregularly is critical for activity transmission between neuronal networks. To quantify the interval variability of the output spike trains, we define the coefficient of variation (C_v) as the ratio of the standard deviation to the mean of the spike interval. If the output firing

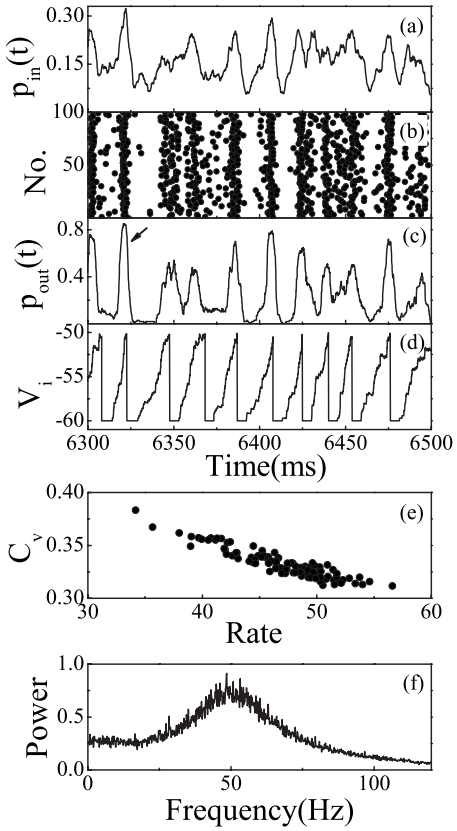

FIG. 2. $R_{in}=31$, $c=0.1$, $S_{in}=0.063$, and $g=60$. (a) The input STH $p_{in}(t)$ versus time. (b) Spike raster plots of the output spike trains. (c) The output STH $p_{out}(t)$ versus time. (d) The membrane potential V_i of one selected output neuron versus time. (e) The coefficient of variation C_v of each neuron versus its firing rate. (f) The power spectrum of $p_{out}(t)$.

rate R_{out} is much smaller, the value of C_v cannot reliably characterize the variability of the output spike trains because of the limited operating time. In this paper, for $R_{out}<1$, we do not compute the value of C_v. The C_v for the whole network is the average value across all neurons. An average over 50 different noise realizations is taken to obtain reported results.

From the viewpoint of nonlinear dynamics, the two-layered network in Fig. 1(a) can be regarded as a nonlinear mapping that maps the firing rate and synchrony (R_{in},S_{in}) in the input layer to (R_{out},S_{out}) in the output layer. In the following we will carry out various numerical experiments to study this mapping, which is expected to depend on the projection strength g.

III. RESULTS

Let us first consider a situation that the input firing rate R_{in} and the projection strength g are large enough. Figure 2(a) shows the STH of the input spike trains with $R_{in}=31$, $c=0.1$, and $g=60$. It can be clearly seen that the fluctuation of the input STH is small since the common noise is only 10% of the whole noise input. The value of the input synchrony S_{in} is only 0.063. Figures 1(b)–1(d) show the corresponding raster plots of the output spike trains, the output STH, and the time series of the membrane potential of one randomly selected output neuron. Obviously, there exists greater synchrony in the output spike trains ($S_{out}=0.48$). The underlying mechanism is interpreted as follows. There are many small peaks in the input STH, which arises from the common noise [see Fig. 2(a)]. By contrast, the flat part is caused by the uncorrelated noise. These uncorrelated input spikes can depolarize the membrane potentials of the postsynaptic neurons to near the firing threshold [compare Figs. 2(a) and 2(d)]. As a result, when those correlated spikes arrive, the postsynaptic neurons can be easily excited to fire. The frequency with which the peaks in the input STH appear is proportional to the input rate R_{in}. Since the input rate R_{in} is large ($R_{in}=31$), the peaks in the input STH occur very frequently, meaning that the period that the neurons stay near the threshold is short. Therefore, the probability that the neurons are depolarized to cross the threshold only by these uncorrelated input spikes is small. Adding up all these factors, the postsynaptic neurons are excited by correlated input spikes with rather large probability and depolarized to fire by uncorrelated input firings with small probability. That is, there exists greater synchrony in the output spike trains. We call such an effect "synchrony amplification effect." Since the membrane potentials of the neurons are required to be depolarized to near the firing threshold by independent input spikes in such an effect, the value of the coupling strength g needs to be large enough. After the neurons fire spikes with great correlation [see the arrow in Fig. 2(c)], the membrane potentials of the neurons are reset to the resting potential and kept at this level during the refractory period [see Fig. 2(d)]. Then they begin to integrate their input spikes to generate the next spike. The time that these neurons need to integrate and pass the threshold is almost the same because the number of the input connections of each neuron is roughly equal. Therefore, there still exists a peak at about 6350 ms in the output STH [see Fig. 2(c)]. Since the neurons need a period of time to integrate input spikes to pass the threshold, there are almost no firings in the process of integration. Due to the fluctuation of the number of the input connection, there exists some difference between the averaged output firing rate of each neuron. With the number of the input connections increasing, the averaged output firing rate of the neurons increases and the coefficient of variation C_v of each neuron decreases [see Fig. 2(e)], which arises from the fact that the neurons with more input connections need less time to integrate and fire more regularly. There is a peak in the power spectrum of the output STH located at about 50 Hz [see Fig. 2(f)], meaning that on average the neurons need about 20 ms to integrate and pass the threshold.

The firing rate R_{out}, the synchrony degree S_{out}, and the coefficient of variation C_v of the output spike trains versus the input synchrony S_{in} for different values of the input firing rate R_{in} are plotted in Figs. 3(a)–3(c), respectively, with $g=60$. Whether the output rate R_{out} increases or decreases with the input synchrony S_{in} depends on the input rate R_{in} [see Fig. 3(a)], which arises from the transition of the working mode of the neurons. This shows that there is nontrivial interplay between firing rate and synchrony. For $S_{in}=0$, the neurons work as temporal integrators [18] and generate

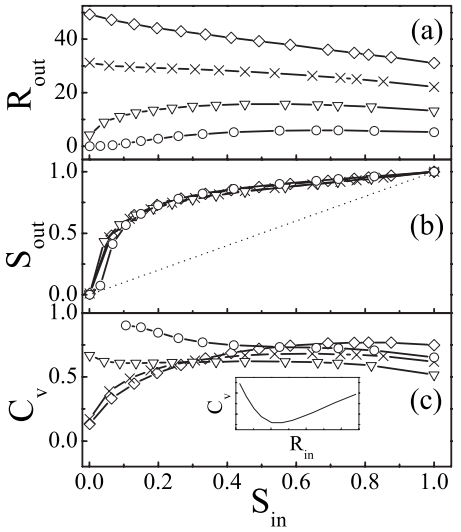

FIG. 3. $g=60$. (a) The output rate R_{out}. (b) The output synchrony S_{out}. (c) The coefficient of variation C_v plotted as a function of the input synchrony S_{in}. Each symbol represents different input rate R_{in}: 5 (○), 13 (▽), 22 (×), and 31 (◇). The dotted line in (b) is the diagonal $S_{in}=S_{out}$. Inset of (c) shows C_v versus R_{in} with $S_{in}=1$.

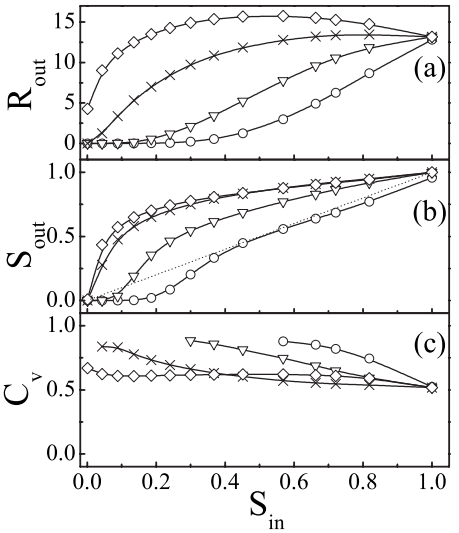

FIG. 4. $R_{in}=13$. (a) The output rate R_{out}. (b) The output synchrony S_{out}. (c) The coefficient of variation C_v plotted as a function of the input synchrony S_{in}. Each symbol represents different coupling strength g: 24 (○), 30 (▽), 45 (×), and 60 (◇). The dotted line in (b) is the diagonal $S_{in}=S_{out}$.

spikes entirely by integrating input spikes. By contrast, for $S_{in}=1$, the neurons act as coincidence detectors [18] and the neuronal activities are fully dominated by the synchronized input meaning $R_{in}=R_{out}$ and $S_{out}=1$. As the input synchrony S_{in} increases from 0 to 1, the working mode of the neurons is gradually changed from temporal integrators to coincidence detectors. As discussed above, due to the synchrony amplification effect, the output synchrony S_{out} increases quite rapidly as the input synchrony S_{in} increases from 0 to 0.1. Such a rapid transition holds true for different input firing rate R_{in} [see Fig. 3(b)]. With the input synchrony S_{in} increasing from 0.1 to 1, the output synchrony S_{out} increases slowly. For intermediate values of the input synchrony S_{in}, these unsynchronous input spikes depolarize gradually the membrane potentials of the postsynaptic neurons while those synchronous packets make the membrane potentials of the postsynaptic neurons increase sharply. The probability that the neurons follow those synchronous packets to fire spikes increases with the input synchrony S_{in}. For large input firing rates without correlation ($R_{in}=22$ or 31), the mean value of the input current far exceeds the firing threshold. As a result, the neurons fire regularly and the value of C_v is much small [see Fig. 3(c)]. Differently, for small input firing rates without correlation ($R_{in}=13$), the average value of the input current is less than the firing threshold and the output spikes are totally caused by the fluctuation of the input current. As a result, the neurons fire spikes with high variability [see Fig. 3(c)]. With fully synchronized input spike trains, since the output spikes totally follow the input firings, the variability of the output spike trains is the same as that of the input spike trains. That is, the coefficient of variation C_v measures the extent of the regularity of the input spikes. It can be seen that, with $S_{in}=1$, both the value of C_v with $R_{in}=5$ and the value of C_v with $R_{in}=31$ are larger than that with $R_{in}=13$ [see Fig. 3(c)]. The relationship between the coefficient of variation C_v and the input rate R_{in} with fully synchronized input is summarized in the inset of Fig. 3(c). The value of C_v first decreases and then increases as the input firing rate R_{in} increases, which arises from a widely investigated effect termed "coherence resonance" (CR) [19,20]. It is believed that CR is caused by different noise dependencies of the activation and the excursion times [19]. For the occurrence of CR, the mean input current I_0 of the presynaptic neurons is needed to be below the threshold [21].

Figure 4 depicts the output rate R_{out}, the output synchrony S_{out}, and the coefficient of variation C_v versus the input synchrony S_{in} for different values of the coupling strengths g with the input rate $R_{in}=13$. For fully synchronized input ($S_{in}=1$), every presynaptic synchronous packet can effectively excite the postsynaptic neurons to fire spikes at the same time exactly. Since the input rate R_{in} of each curve is the same, all the output rate curves evolve to the same point as the input synchrony S_{in} increases [see Fig. 4(a)]. For $g=60$, the output synchrony S_{out} increases sharply as the input synchrony S_{in} increases from 0 to 0.1, which arises from the synchrony amplification effect as discussed above. However, with the coupling strength g decreasing, such a rapid transition gradually disappears [see Fig. 4(b)]. The underlying reason is that, for small coupling strength g, the average input current is small. As a result, the membrane potentials of the neurons cannot be depolarized to near the threshold by uncorrelated spikes and the postsynaptic spikes are mainly excited by presynaptic synchronous packets, which results in that the neurons discharge spikes with large variability [see Fig. 4(c)]. Since the membrane potentials are required to fluctuate near the threshold in the synchrony amplification effect, there exists no a rapid transition in the output synchrony curve.

We would like to stress the nontrivial mapping from (R_{in},S_{in}) to (R_{out},S_{out}) at a relatively small projection strength g, e.g., $g=30$. There is a critical value of S_{in} as indicated by the intersection of the curve of S_{out} with the

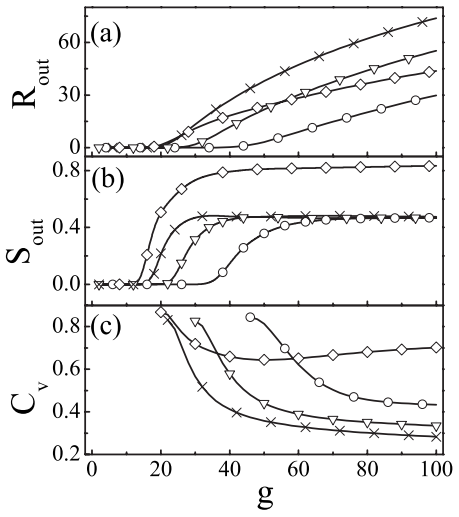

FIG. 5. (a) The output rate R_{out}. (b) The output synchrony S_{out}. (c) The coefficient of variation C_v plotted as a function of the coupling strength g. Each symbol represents different input parameters: R_{in}=13, c=0.1, and S_{in}=0.043 (○); R_{in}=22, c=0.1, and S_{in}=0.057 (▽); R_{in}=31, c=0.1, and S_{in}=0.063 (×); and R_{in}=22, c=0.6, and S_{in}=0.372 (◇).

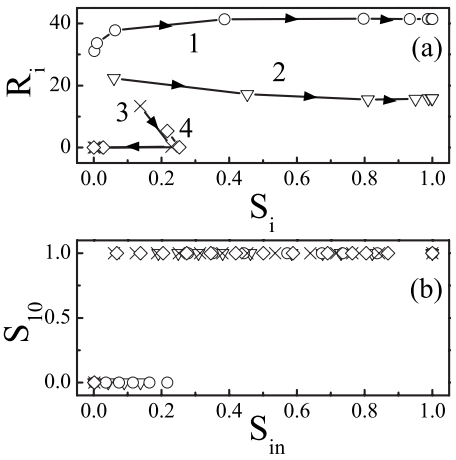

FIG. 6. (a) Each curve represents different parameters: R_{in}=31, c=0, S_{in}=0, and g=45 (○); R_{in}=22, c=0.1, S_{in}=0.057, and g=45 (▽); R_{in}=13, c=0.3, S_{in}=0.134, and g=30 (×); and R_{in}=5, c=0.5, S_{in}=0.199, and g=30 (◇). The layer index increases along the direction of the arrows. (b) The synchrony S_{10} versus the input synchrony S_{in} with g=30. Each symbol represents different input rate R_{in}: 5 (○), 13 (▽), 22 (×), and 31 (◇).

dotted diagonal line in Fig. 4(b). The synchrony in the output is enlarged when S_{in} is larger than this value and is reduced otherwise. However, the output rate R_{out} is significantly reduced in a broad range of S_{in}. As we will discuss later, when the mapping between (R_{in},S_{in}) to (R_{out},S_{out}) is iterated in the feedforward network, the synchrony can first increase but will eventually decrease to zero due to a significantly reduced firing rate and the neurons in deep layers cannot be activated.

Figure 5 shows how the input spike trains are transmitted by the network as the coupling strength g increases. For the four selected parameters of the input spike trains, every curve shows a threshold-and-linear relationship between the output rate R_{out} and the coupling strength g [see Fig. 5(a)]. For small coupling strength g, only these synchronous packets can effectively induce postsynaptic firings. Differently, for large coupling strength g, the neurons discharge spikes mainly by temporal integration. Therefore, with identical input rate (R_{in}=22), as the coupling strength g increases, the output rate R_{out} with great input synchrony (S_{in}=0.372) is first larger than that with less input synchrony (S_{in}=0.057) and then vice versa [see Fig. 5(a)]. With the coupling strength g increasing, the output synchrony S_{out} increases sharply and then saturates at a value, which is caused by the synchrony amplification effect [see Fig. 5(b)]. Since the membrane potentials of the neurons are required to be depolarized to near the threshold in the synchrony amplification effect, there still exists such an effect when the coupling strength g is large. The saturated value of the output synchrony S_{out} increases with the input synchrony S_{in} (compare the two curves with the input rate R_{in}=22). With the coupling strength g increasing, the average value of the input current increases. Therefore, the neurons fire spikes more regularly and the coefficient of variation C_v decreases [see Fig. 5(c)]. For small input firing rate R_{in}, the mean value of the input current increases slowly with the coupling strength g, which results in that the output synchrony S_{out} increases slowly [see Fig. 5(b)]. With great synchrony S_{in}, the neurons fire spikes still with large variability because the presynaptic neurons discharge spikes quite irregularly and these input synchronous packets can induce postsynaptic firings effectively [see Fig. 5(c)]. For large coupling strength g, since the fluctuation amplitude of the input current decreases with the input rate R_{in}, the value of C_v with large R_{in} is less than that with small R_{in} [see Fig. 5(c)]. These results again show clearly that the mapping from (R_{in},S_{in}) to (R_{out},S_{out}) depends strongly on the projection strength g.

The multilayer feedforward network has become a research focus in the field of theoretical neuroscience recently [8–11,22]. To investigate how spike trains are transmitted in such a network, we construct a ten-layer feedforward network with 2000 IF neurons in each layer. Each neuron randomly receives synaptic inputs from about 5% of all the neurons in the previous layer. There exist no connections between the neurons in the same layer. Figure 6(a) shows how the firing rate R_i and the synchrony S_i of layer i evolve in the process of neuronal activity transmission. Each curve with different symbols represents different coupling strength g, input rate R_1, and input synchrony S_1; the first point of each curve is (S_1,R_1) of layer 1 and the second point is (S_2,R_2) of layer 2, and so on. Following the direction of the arrows, the layer index increases. In such an architecture network, the output spike trains of layer 1 are injected to layer 2 and then the output spike trains of layer 2 are projected to layer 3. Thus, transmission of spike trains in the feedforward network can be roughly regarded as an iteration process of the relationship between input and output spike trains. For the four selected input parameters, the activity in layer 10 is none (lines 1 and 2) or in full synchrony (lines 3 and 4). From the mapping between two layers in Fig. 4(b), we can see that only two fixed points (S=0 and S=1) are

stable after many iterations, which is confirmed by simulations with different input parameters [see Fig. 6(b)]. It is worth noting that synchrony can be gradually built up in deep layers even if there is no correlation between input spike trains [see curve 1 in Fig. 6(a)], which also appears in networks of Hodgkin-Huxley neurons [10]. Full synchrony is the default state of the deep layers in the feedforward network when the input rate and projection strength g are large enough. With independent noise injected to each layer, very many layers are needed to achieve full synchrony and the input signal can be stably transmitted [8]. On the other hand, enhanced synchrony can be accompanied by significantly reduced firing rate in the first few layers and the activity cannot propagate to deeper layers [the cases of 3 and 4 in Fig. 6(a)]. There are also situations where both R and S decrease monotonically when the initial values are small enough (not shown in the figure).

IV. DISCUSSION AND CONCLUSION

To conclude, we have explored the $2D$ space (rate and synchrony) mapping between input and output spike trains of a neuronal network. As the input synchrony increases, the neurons first work as temporal integrators and then gradually as coincidence detectors. With enough large coupling strength, even if there is a small correlation between input spike trains, the output spike trains can exhibit great synchrony, which is caused by the synchrony amplification effect. For small coupling strength, such an effect disappears because the membrane potentials of the postsynaptic neurons cannot be depolarized to near the firing threshold. With the coupling strength increasing, the output synchrony increases sharply and then saturates at a large value. The results reveal nontrivial interplay between firing rate and synchrony, which depend crucially on the projection strength. Transmission of neuronal activity in the feedforward network can be approximately regarded as an iteration process of the input-output relationship of one network. The activity in deep layers can only be none or in full synchrony depending on the input parameters due to the interplay between firing rate and synchrony.

Since information is contained in spikes trains in the nervous system, our results provide insights on how information is transmitted by neuronal networks. However, there usually exist couplings between neurons in the nervous system. Whether two neurons are connected depends on the cell type, the distance between neurons, the extent of common excitatory input [23], and so on. It deserves a further study to investigate what is the relationship between input and output spike trains when the neurons are coupled with each other in a biological way. Inhibitory neurons are not included in this paper. What functional roles the inhibitory neurons play in the transmission of spike trains is an ongoing work. Adaptation has been observed in many sensory systems including the visual system [24], olfactory system [25], etc. It is an interesting topic to investigate the input-output relationship of spike trains in a network where the neuronal activity can be adapted to external stimulus.

ACKNOWLEDGMENTS

This work was supported by Hong Kong Baptist University and NNSFC Grant No. 10804013 (S.W.).

[1] R. C. deCharms and A. Zador, Annu. Rev. Neurosci. **23**, 613 (2000); M. I. Rabinovich, P. Varona, A. I. Selverston, and H. D. I. Abarbanel, Rev. Mod. Phys. **78**, 1213 (2006).
[2] J. de la Rocha, B. Doiron, E. Shea-Brown, K. Josic, and A. Reyes, Nature (London) **448**, 802 (2007).
[3] E. Shea-Brown, K. Josic, J. de la Rocha, and B. Doiron, Phys. Rev. Lett. **100**, 108102 (2008).
[4] S. Neuenschwander, M. Castelo-Branco, J. Baron, and W. Singer, Philos. Trans. R. Soc. London, Ser. B **357**, 1869 (2002).
[5] M. N. Shadlen and J. A. Movshon, Neuron **24**, 67 (1999).
[6] X. Li and G. A. Ascoli, Neural Comput. **20**, 1717 (2008).
[7] M. Diesmann, M. Gewaltig, and A. Aertsen, Nature (London) **402**, 529 (1999); M. Gewaltig, M. Diesmann, and A. Aertsen, Neural Networks **14**, 657 (2001); H. Cateau and T. Fukai, *ibid.* **14**, 675 (2001).
[8] M. C. W. V. Rossum, G. G. Turrigiano, and S. B. Nelson, J. Neurosci. **22**, 1956 (2002).
[9] A. Reyes, Nat. Neurosci. **6**, 593 (2003); B. Doiron, J. Rinzel, and A. Reyes, Phys. Rev. E **74**, 030903 (2006); H. Cateau and A. D. Reyes, Phys. Rev. Lett. **96**, 058101 (2006); S. Goedeke and M. Diesmann, New J. Phys. **10**, 015007 (2008).
[10] S. Wang, W. Wang, and F. Liu, Phys. Rev. Lett. **96**, 018103 (2006).
[11] S. Wang and W. Wang, Neuroreport **16**, 807 (2005).
[12] E. Zohary, M. N. Shadlen, and W. T. Newsome, Nature (London) **370**, 140 (1994); J. Alonso, W. M. Usrey, and R. C. Reid, *ibid.* **383**, 815 (1996); W. Bair, E. Zohary, and W. T. Newsome, J. Neurosci. **21**, 1676 (2001).
[13] P. N. Steinmetz *et al.*, Nature (London) **404**, 187 (2000).
[14] M. Stopfer, S. Bhagavan, B. H. Smith, and G. Laurent, Nature (London) **390**, 70 (1997).
[15] S. Wang, F. Liu, W. Wang, and Y. Yu, Phys. Rev. E **69**, 011909 (2004).
[16] A. Tonnelier and W. Gerstner, Phys. Rev. E **67**, 021908 (2003); A. Roxin, H. Riecke, and S. A. Solla, Phys. Rev. Lett. **92**, 198101 (2004); R. Moreno-Bote and N. Parga, *ibid.* **96**, 028101 (2006).
[17] X. Pei, L. Wilkens, and F. Moss, Phys. Rev. Lett. **77**, 4679 (1996); S. Wang, J. Xu, F. Liu, and W. Wang, Eur. Phys. J. B **39**, 351 (2004); S. Wang and C. Zhou, Phys. Rev. E **79**, 061910 (2009).
[18] P. Konig, A. K. Engel, and W. Singer, Trends Neurosci. **19**, 130 (1996).
[19] A. S. Pikovsky and J. Kurths, Phys. Rev. Lett. **78**, 775 (1997).
[20] A. Longtin, Phys. Rev. E **55**, 868 (1997); C. Zhou, J. Kurths, and B. Hu, Phys. Rev. Lett. **87**, 098101 (2001).
[21] B. Lindner, L. Schimansky-Geier, and A. Longtin, Phys. Rev.

E **66**, 031916 (2002).

[22] V. Litvak, H. Sompolinsky, I. Segev, and M. Abeles, J. Neurosci. **23**, 3006 (2003); J. Li, F. Liu, D. Xu, and W. Wang, Europhys. Lett. **85**, 38006 (2009).

[23] Y. Yoshimura, J. L. M. Dantzker, and E. M. Callaway, Nature (London) **433**, 868 (2005).

[24] D. Chander and E. J. Chichilnisky, J. Neurosci. **21**, 9904 (2001).

[25] A. R. Best and D. A. Wilson, J. Neurosci. **24**, 652 (2004).